J. Physiol. (1981), **318**, *pp.* 297–316
With 10 *text-figures*
Printed in Great Britain

EVIDENCE FOR THE EXISTENCE OF THREE TYPES OF POTASSIUM CHANNELS IN THE FROG RANVIER NODE MEMBRANE

BY J. M. DUBOIS

From the Laboratoire de Neurobiologie, Ecole Normale Supérieure, 46, rue d'Ulm, 75230 Paris Cedex 05, France

(*Received 6 August 1980*)

SUMMARY

1. In voltage clamped myelinated fibres, the K^+ current was recorded in high-K^+ media to allow analysis without complications due to K^+ accumulation.

2. After a depolarization, the tail of K^+ current following repolarization decreases in two phases: a fast phase lasting about 20 msec and a slow exponential phase lasting several hundred milliseconds. When the duration of the depolarization is increased, the amplitude at time zero of the fast phase increases (activation of the conductance) and then decreases slowly (inactivation of the conductance). Simultaneously, the amplitude of the slow phase, extrapolated to time zero of repolarization, increases slowly and reaches a steady-state level (about 20 % of the maximum instantaneous current) after about 600 msec of depolarization.

3. The fast phase of the tail current is blocked by external application of 4-aminopyridine (4-AP) ($K_D = 10^{-5}$ M). The slow phase is unaltered by 4-AP ($10^{-7} - 10^{-2}$ M).

4. In the presence of 4-AP (10^{-3} M), the remaining slow K^+ current, activated by depolarizations, does not inactivate.

5. During depolarizations and repolarizations, the conductance of the slow current (G_{Ks}) varies exponentially. The steady-state value of the slow conductance and its time constant of activation vary with voltage. The variation of the slow conductance with time and voltage can be described by a closed–open model, assuming that each channel is gated by one particle. The activation kinetics of the slow current is unaltered by long lasting (500 msec) prepolarizations.

6. The fast K^+ conductance, calculated from the fast tail current, is fully inactivated at the end of a 3 min depolarization to 0 mV.

7. The fast K^+ conductance can be decomposed into two components: one component (G_{Kf_1}) activating between −80 and −30 mV and inactivating very slowly ($\tau = 45$ sec at $E = 0$ mV); one component (G_{Kf_2}) activating between −40 mV and +30 mV and inactivating slowly ($\tau = 2$ sec at $E = 0$ mV). $t = 12$ °C.

8. The maximum slow and fast conductances increase with $[K]_o$. While the maximum fast conductance tends to saturate at high external K^+ concentrations, the maximum slow conductance shows no sign of saturation.

9. A comparison between motor and sensory fibres shows that, while the amplitude of maximum slow and fast conductances are identical for both types of fibres, the

amplitude of fast-1 conductance is larger and consequently the amplitude of fast-2 is smaller in motor than in sensory fibres. The different spike frequency adaptations observed on both types of fibres are discussed in relation to these different relative fast conductances amplitudes.

10. It is concluded that the K^+ conductance of the nodal membrane is composed of three components (G_{Ks}, G_{Kf_1} and G_{Kf_2}) corresponding to three different and distinct types of K^+ channels.

INTRODUCTION

In the preceding paper (Dubois, 1981), it was noted that on repolarization the K^+ conductance in the nodal membrane turns off with a large and fast phase followed by a slow phase which lasts for several hundred milliseconds. This observation may suggest that the membrane contains different classes of K^+ channels. The hypothesis of the existence, within the nodal membrane, of different types of K^+ channels has already been proposed by several authors (Schwarz & Vogel, 1971; Palti, Ganot & Stämpfli, 1976; Van den Berg, Siebenga & De Bruin, 1977; Ilyin, Katina, Lonskii, Makovsky & Polishchuk, 1977; Krylov & Makovsky, 1978). Schwarz & Vogel (1971) showed that the stationary inactivation of I_K remains incomplete even with large depolarizing pulses. Moreover, they showed that the inactivation of I_K develops in two phases (fast and slow inactivation). On the basis of K^+ current noise analyses, Van den Berg *et al.* (1977) showed that both the affinities for tetraethylammonium and the voltage dependent properties of K^+ channels are different after depolarizations lasting either 400 msec or 60 sec. Ilyin *et al.* (1977) showed that in isotonic KCl solution, the tail of K^+ current upon repolarization after conditioning depolarizations of various amplitudes and durations can be decomposed into two exponential functions of time (I_{K1} and I_{K2}). I_{K1} inactivates with inreasing duration of the conditioning depolarization whereas I_{K2} does not. All these observations suggest that the K^+ conductance is composed of more than one component. The aim of this paper is to decompose the K^+ conductance into independent components and to study the properties of each component with respect to voltage, time and K^+ concentration.

METHODS

All methods were as described in the preceding paper (Dubois, 1981). The experiments were carried out on fibres in which no noticeable change in the instantaneous reversal potential could be observed in K-rich media.

Most of the data presented are based on instantaneous measurements of the tail K^+ current occurring on repolarization after conditioning depolarizations used to activate the current. The capacity current was automatically compensated for. Since the conductance changes slowly compared to the time required to change the membrane to a new potential level (about 20 μsec), the initial part of the tail current (peak of the tail current) was considered as the instantaneous value of the tail current (see Methods in the preceding paper). These K^+ current values are referred to as 'instantaneous currents'. The values obtained by extrapolating the later part of the tail current to the time zero of repolarization are referred to as the 'instantaneous extrapolated currents'.

RESULTS

Slow component of the tail current

At repolarization, the K^+ conductance, activated by a conditioning depolarizing pulse deactivates in two phases: a fast and a slow one (see Fig. 7 of the preceding paper and Ilyin *et al.* 1977). The question arises as to whether the slow and fast components are related or not. In other words, do the slow and fast components

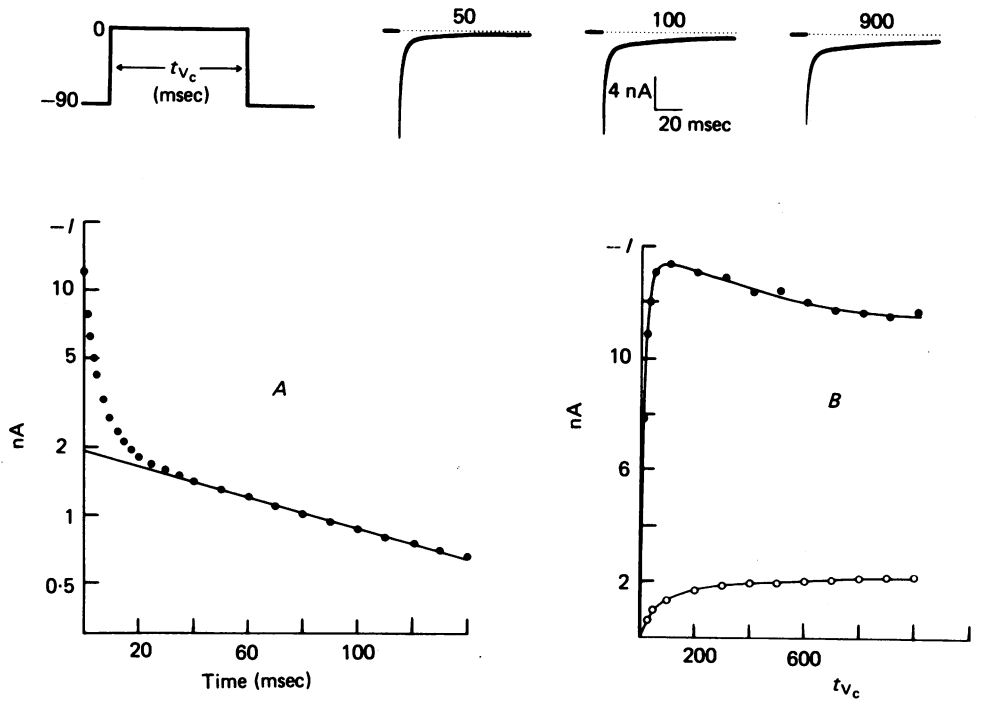

Fig. 1. The tail current was recorded in 117 mM-K at $E = -90$ mV after activation of the conductance by conditioning depolarizations (V_c) of various durations to $E = 0$ mV.

Upper: tail currents recorded after depolarizations of 50, 100, 900 msec. The longer the depolarization, the smaller the initial peak of current and the larger the slow phase of the tail current.

Lower: *A*, semilogarithmic plot of the decay of the tail current after a conditioning depolarization lasting 100 msec. The slow phase can be described by an exponential function of time (straight line). *B*, instantaneous extrapolated slow phase (○) and initial peak (●) of tail current as a function of conditioning depolarization duration. While the amplitude of the instantaneous extrapolated slow phase increases slowly with the duration of the depolarization, the initial peak decreases after a fast activation. Fibre: 25–1–9.

correspond to distinct classes of K^+ channels, or reflect a multistep shutting off of only one type of K^+ channels? The following experiment was undertaken to answer this question. To avoid complications due to changes in driving force resulting from an accumulation (or depletion) of K^+ ions outside the membrane, the conductance was activated by conditioning depolarizing pulses (V_c) to 0 mV in isotonic KCl solutions. In these conditions, the K^+ current is nil and the K^+ equilibrium potential potential E_K is necessarily constant during the conditioning depolarization.

Furthermore, it was assumed that the tail current arising at repolarization does not induce changes in E_K and consequently the time course of the tail current reflects faithfully the time course of the conductance change (see Fig. 7*B* of the preceding paper).

The tail current was recorded at the holding potential (−90 mV) after activation of the conductance by conditioning pulses of various durations. One can observe (Fig. 1) that with longer conditioning pulses, the slow component of the tail current increases while the total peak of the tail current decreases. Plotting the tail current on semi-logarithmic coordinates (Fig. 1*A*) shows that the time course of the slow component can be described by a single exponential function of time. The extrapolated value of the straight line to time zero of repolarization corresponds to the instantaneous value of the slow component of the tail current and, owing to the approximate linearity of the instantaneous current–voltage relationships (Dubois & Bergman, 1977; Attwell, Dubois & Ojeda, 1980), is proportional to the slow component of the K^+ conductance at the end of the conditioning depolarization. Similarly, the peak of the tail current is proportional to the total K^+ conductance at the end of the conditioning depolarization, Increasing the duration of V_c, one can see (Fig. 1*B*) that the slow instantaneous component of the tail current increases very slowly to reach a steady-state level for V_c durations of about 600 msec. In contrast, the total instantaneous current reaches a maximum value for V_c durations of 50–100 msec and then decreases beyond 600 msec.

These results agree with the data of Ilyin *et al.* (1977) and strongly suggest that the slow component of the K^+ conductance corresponds to slow K^+ channels distinct from the familiar fast K^+ channels. However, the demonstration of the existence of two distinct K^+ channels is not entirely convincing until one of the two components is blocked specifically. For this purpose, 4-aminopyridine (4-AP), which is known to affect specifically the K^+ conductance of the squid axon membrane (Yeh, Oxford, Wu & Narahashi, 1976; Meves & Pichon, 1977) and the frog nodal membrane (Ulbrich & Wagner, 1976), was found to be an efficient tool.

Pharmacological separation of fast and slow K^+ conductances

In the experiment presented in Fig. 2, 4-AP (10^{-7}–10^{-2} M) was added to the external isotonic K^+ solution. In each solution, the tail of K^+ current was recorded at the holding potential −90 mV after activation of the conductance by a single 100 msec depolarizing pulse to $E = 0$ mV. The slow component of the tail current was extrapolated to time zero of repolarization. The instantaneous fast component was calculated as the difference between the total peak of current and the instantaneous extrapolated value of the slow component. Whereas the fast component is blocked by 4-AP with an apparent dissociation constant of 10^{-5} M, the slow component remains unaltered even with 4-AP concentrations (10^{-3}, 10^{-2} M) which completely block the fast component.

From this experiment, it can be concluded that the K^+ conductance of the nodal membrane is composed of (at least) two components corresponding to two different classes of K^+ channels. In the presence of 10^{-3} or 10^{-2} M-4-AP, the block of the fast component is not removed by repetitive pulsing. In such conditions, the slow component can be studied separately.

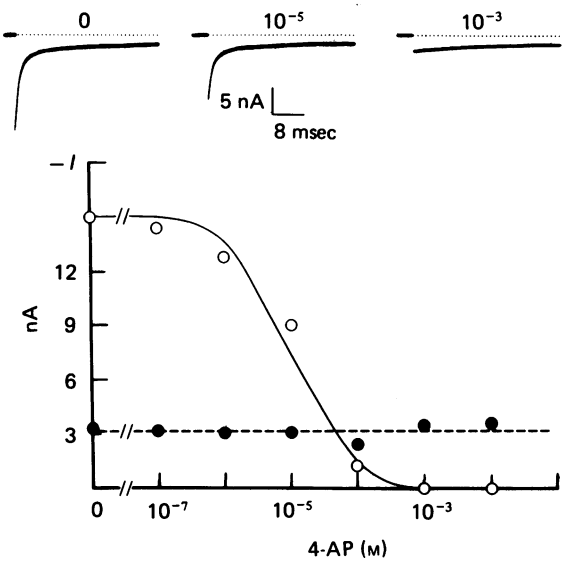

Fig. 2. The tail current was recorded in 117 mM-K at $E = -90$ mV after a 100 msec conditioning depolarization to 0 mV.

Upper: tail currents in the presence of 0, 10^{-5} and 10^{-3} M-4-AP.

Lower: instantaneous extrapolated slow phase (●) and instantaneous fast phase (○) calculated as the difference between the initial peak of the tail current and the instantaneous (extrapolated) slow phase of the tail current as a function of the logarithm of 4-AP concentration. While the amplitude of the slow phase is unaltered by 4-AP at concentrations varying between 10^{-7} and 10^{-2} M, the fast phase is decreased by 4-AP and completely blocked by 4-AP concentrations equal to or greater than 10^{-3} M. The curve represents the inhibition of the fast phase assuming a one to one reaction between channels and 4-AP molecules with a dissociation constant of 10^{-5} M. Fibre: 10–4–9.

Properties of the slow K^+ channels

The slow K^+ current was recorded in isotonic K^+ solutions containing 1 mM-4-AP (Fig. 3). In the absence of 4-AP, the slow K^+ current is present with the fast one (Fig. 3*A*, *B*). It does not however contribute significantly to the initial rise of current during depolarization (Fig. 3*A*). At repolarization, the tail current recorded in the presence of 4-AP corresponds to the slow phase of the current recorded in absence of 4-AP (Fig. 3*B*) and decreases exponentially (Fig. 3*C*). During long lasting depolarizations (Fig. 3*D*), the slow K^+ current does not inactivate. It is inward for negative membrane potentials, reverses its direction at $E = 0$ mV and increases with increased positive voltages.

The instantaneous slow current–voltage curve appears to be linear in high or low K^+ solutions. Thus, the conductance can be used as an expression of the permeability state of the membrane. The slow conductance (G_{Ks}) was calculated as a function of voltage and time in external solutions containing either 117 or 60 mM-K (Fig. 4). The steady-state slow conductance (G_{Ks_∞}) increases with depolarization and saturates near 0 mV (Fig. 4*A*). It increases with external K^+ concentration (Fig. 4*A*) without modification of its voltage dependence (Fig. 4*B*) or its time dependence (Fig.

4 *C*, *D*, *E*). The kinetics of the conductance change activation and deactivation) can be described by an exponential (Fig. 4*C*, *D*) whose time constant varies with voltage (Fig. 4*E*).

The fact that the slow conductance activates exponentially and saturates for large depolarizations suggests that the kinetic properties of the slow K^+ channels can be described by a two-state model according to the scheme

$$S_c \underset{\beta_s}{\overset{\alpha_s}{\rightleftharpoons}} S_o,$$

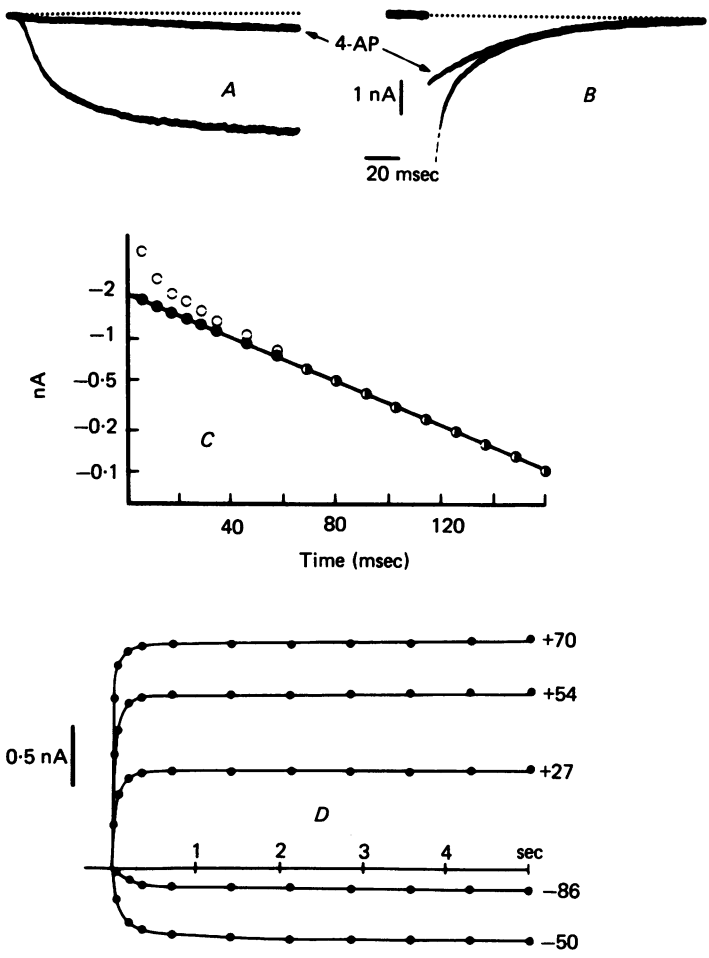

Fig. 3. *A*, superposition of K^+ current traces recorded during depolarizations to E = −40 mV in 117 mM-K and 117 mM-K + 4-AP (1 mM). *B*, superposition of K^+ current traces (tail currents) recorded at −90 mV after a 100 msec conditioning depolarization to *E* = 0 mV in 117 mM-K and 117 mM-K + 4-AP (1 mM). The tail current in 117 mM-K is partially represented in the Figure. Fibre: 24–6–0. *C*, semilogarithmic plot of the tail currents (presented in *B*) recorded in 117 mM-K (○) and 117 mM-K + 4-AP (●). *D*, slow current recorded in 117 mM-K + 4-AP (1 mM) during depolarizations of different amplitudes (absolute voltage indicated at the end of each curve). Note that the slow current does not inactivate even at large positive potential. Holding potential: −90 mV. Fibre: 30–4–9.

where S_c and S_o correspond respectively to closed and open channels, α_s and β_s being the voltage dependent rate constants of the transition. According to this model, the conductance is proportional to the number of channels in the open configuration. Thus

$$G_{Ks} = s\bar{G}_{Ks},$$

where $\bar{G}_{Ks}$ is the maximum slow conductance (function of $[K]_o$) and s is the proportion of channels in the open configuration.

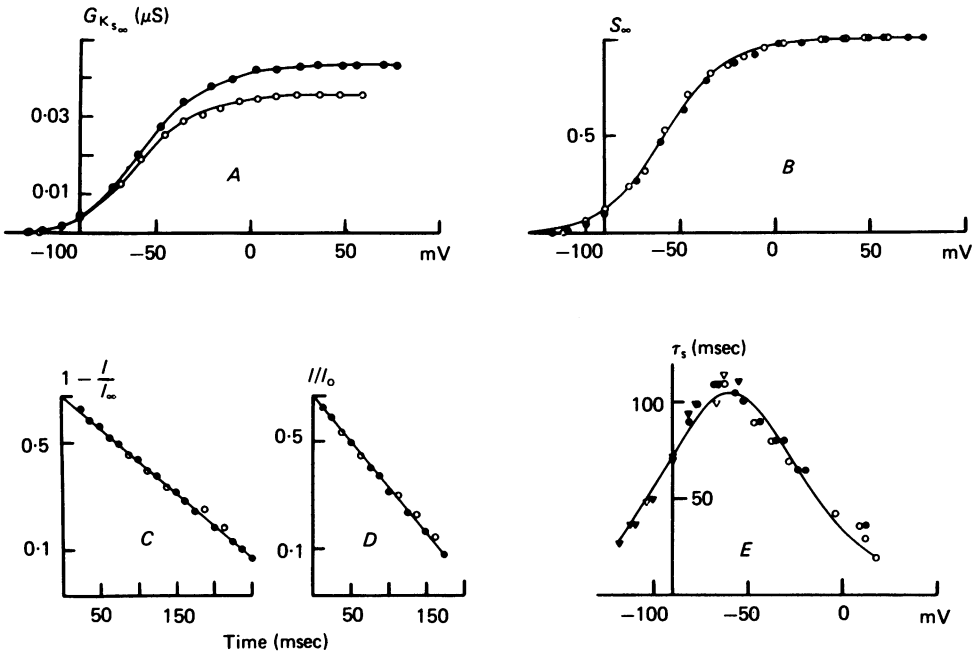

Fig. 4. The slow K^+ current was recorded in 117 mM-K + 4-AP (1 mM) (filled symbols) and 60 mM-K + 4-AP (1 mM) (open symbols) either during depolarizations and hyperpolarizations from a holding potential of −90 mV or during post pulses of different amplitudes after activation of the conductance by a 800 msec depolarization to 0 mV. *A*, steady-state slow condutance *vs.* voltage. *B*, steady-state activation parameter of the slow conductance versus voltage calculated from the data of *A*. *C* and *D*, semilogarithmic plots of the activation (*C*) and deactivation (*D*) of the slow conductance. The voltage was −40 mV in *C* and −90 mV in *D*. *E*, time constant of the activation variable for the slow conductance as a function of voltage. The time constant was calculated either from the on-responses (circles) or from the off-responses (triangles). The curves in B and *E* were calculated using the expressions: $\alpha = 0{\cdot}028\,e^{E/33}$ and $\beta = 0{\cdot}0008\,e^{-E/33}$. Temperature: 12 °C. Fibre: 25–4–9*b*.

The values of α_s and β_s were determined from the variation of s_∞ and τ_s with voltage. In the typical experiment presented Fig. 4, s_∞–V and τ_s–V curves (Fig. 4*B*, *E*) were fitted with

$$\alpha_s = 0{\cdot}028\ e^{E/33},$$
$$\beta_s = 0{\cdot}0008\ e^{-E/33},$$

where *E* is the absolute membrane potential expressed in millivolts.

In different preparations, evidence has been presented of the existence of K^+ channels activated by intracellular Ca and consequently by the Ca influx (see Meech, 1978). Attempts were made to see whether, in the Ranvier node, similar conclusions could be reached for one or both of the K^+ components. Any putative inward Ca-current (never seen in this preparation), and the internal Ca^+

concentration were tentatively altered either by changing the external Ca^+ concentration or by addition of Co^{2+}, Cd^{2+}, quinine (see Atwater, Dawson, Ribalet & Rojas, 1979) (1 mM) and the Ca ionophore (Ro 2–2985/1) to the external solution. These agents did not alter specifically any of the K^+ components in a way which would allow one to conclude that some K^+ channels are activated by intracellular calcium. It is concluded that the different K^+ channels of the nodal membrane are not triggered by internal calcium.

Lack of effect of prepulse on the slow conductance kinetics

It is well known that hyperpolarizing prepulses delay the activation of the classical K^+ current (mainly flowing through fast K^+ channels) (Cole & Moore, 1960; Palti, *et al.* 1976; Begenisich, 1979; Dubois, 1981). It was of interest to known whether prepolarization has an effect of the slow K^+ current. To answer this question, the slow

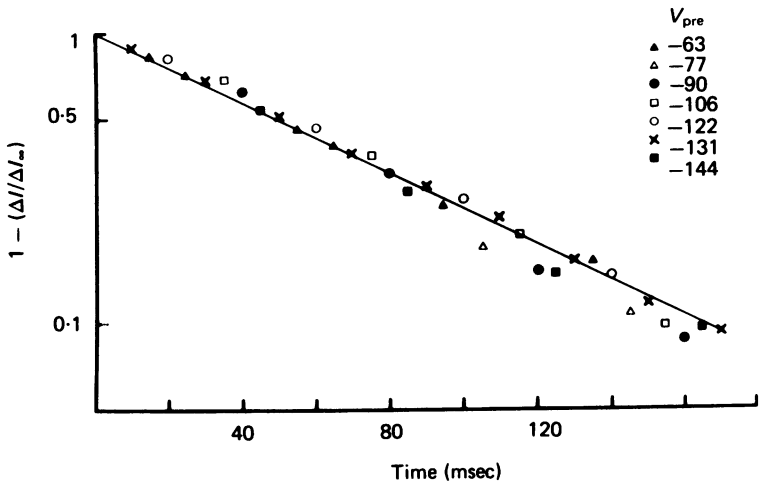

Fig. 5. Semilogarithmic plot against time of the slow current activation recorded at −40 mV, after 500 msec prepulses of various amplitudes. The experimental points are distributed along a straight line which crosses the ordinate axis at time zero. In contrast to the total K^+ current (which mainly consists of the fast current) (see Fig. 6 of the preceding paper), the slow K^+ current is not delayed by a hyperpolarizing prepulse. Fibre: 10–5–9.

K^+ current was recorded in isotonic K^+ Ringer + 1 mM-4-AP during a test pulse to $E = -40$ mV with a 500 msec prepulse of varying amplitude. In Fig. 5, the time dependent current is plotted against time on semilogarithmic co-ordinates. The results show that, within a few milliseconds of uncertainty, the kinetics of the slow current are essentially independent of the prepulse amplitude.

Inactivation of the fast K^+ component

Schwarz & Vogel (1971) observed that for large and long lasting depolarizations, about 20% of the K^+ current does not inactivate. The preceding results raises the possibility that the non-inactivatable K^+ current flows through slow K^+ channels. If so, this would indicate that the fast K^+ current can be completely inactivated during large and long lasting depolarizations. The following experiment was undertaken to test this hypothesis.

The tail current was recorded in isotonic K^+ Ringer at −90 mV after conditioning

depolarizations to $E = 0$ mV of various durations (Fig. 6). The instantaneous value of the fast K^+ current was calculated as the difference between the peak of the tail current and the instantaneous value of the slow K^+ current obtained by extrapolation to time of repolarization of the slow phase of the tail current. Whereas the slow K^+ tail current was constant for pulse durations from 2 to 180 sec, the fast K^+ current declined continuously during this period and was completely inactivated for conditioning depolarizations lasting 180 sec (Fig. 6). This result is in agreement with the hypothesis proposed above and supports the view that the two phases of the tail current reflect the shutting off of two distinct populations of K^+ channels.

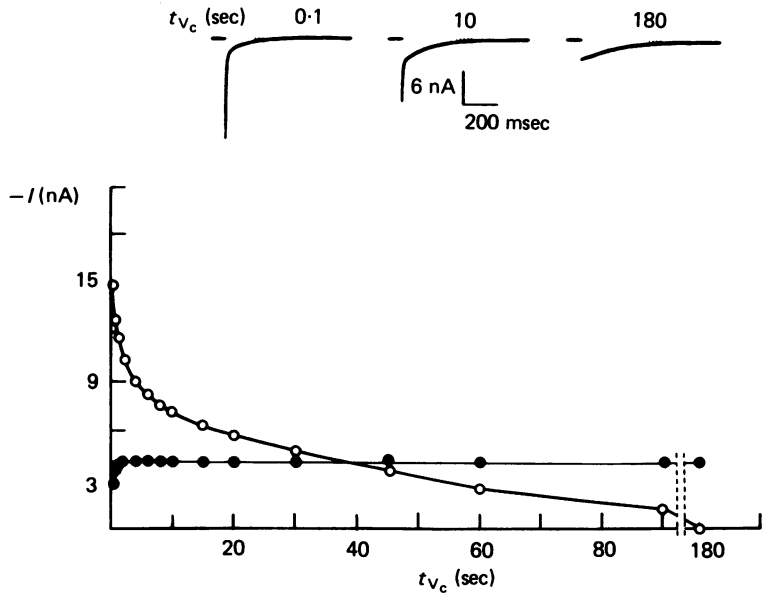

Fig. 6. The tail current was recorded in 117 mM-K at E = −90 mV after conditioning depolarizations to $E = 0$ mV of various durations.

Upper: tail currents recorded after 100 msec, 10 sec and 3 min conditioning depolarizations (V_c).

Lower: instantaneous values of the extrapolated slow phase (●) and instantaneous fast phase (○) (calculated as the difference between the initial peak of the tail current and the instantaneous extrapolated slow phase) versus the duration of the conditioning depolarization. While the slow conductance does not inactivate, the fast one is completely inactivated at the end of a 3 min depolarization to $E = 0$ mV. Fibre: 7–6–9.

Evidence for the existence of two fast K^+ conductances

At the present time, no pharmacological agent has been found to specifically block the slow K^+ current. Consequently, the fast K^+ conductance was calculated from the fast component of the tail current, after subtraction of the slow current from the total tail current. This subtraction can be achieved in two ways. The first is to subtract the slow K^+ current recorded in isotonic KCl Ringer + 4-AP from the total tail current recorded in isotonic KCl Ringer. The second method was that used in the experiments presented in Figs. 2 and 6 and consists of subtracting the extrapolated slow tail current from the total tail current. The time required to obtain experimental data with the

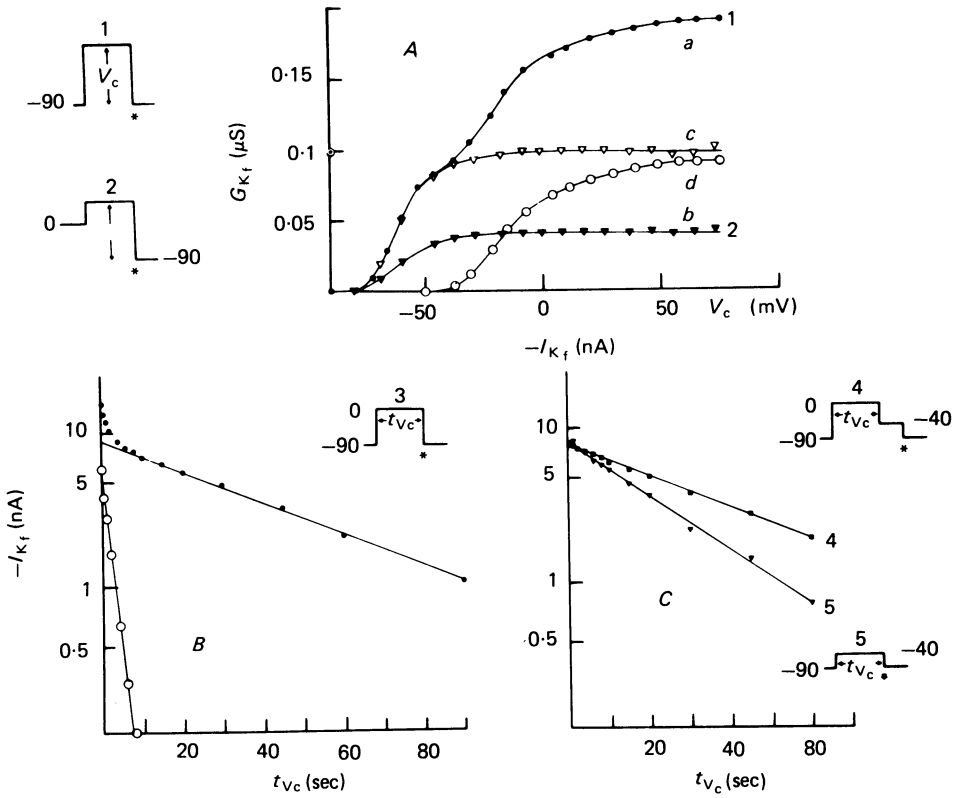

Fig. 7. The fast K^+ conductance was calculated in 117 mM-K from instantaneous fast currents (total instantaneous current minus instantaneous extrapolated slow tail current) recorded at −90 mV (stars in pulse protocols) after activation of the conductances by conditioning depolarizations of various amplitudes and durations. *A*, curve *a* (●): fast conductance–voltage curve calculated from currents recorded using pulse protocol 1. Curve *b* (▲): fast conductance–voltage curve calculated from currents recorded using pulse protocol 2. Curve *c* (△): curve *b* scaled by 2·4 so as to be superimposed on curve *a* between −90 and −40 mV. Curve *d* (○): difference between curves *a* and *c*. *B*, semilogarithmic plot of the inactivation time course of the fast conductance calculated from fast instantaneous currents recorded using pulse protocol 3. The inactivation can be described by the sum of two exponential functions of time. ● give the overall current and ○ give the current remaining after subtracting the slow exponential component (straight line through ●). *C*, semilogarithmic plot of the inactivation time course of the fast conductance calculated from fast instantaneous currents recorded using pulse protocols 4 and 5. In both cases, the inactivation can be described by only one exponential function of time.

The fast conductance–voltage curve (*A* curve *a*) can be decomposed into two components: a component which inactivates with a time constant of 45 sec at $E = 0$ mV (curve *c*) and corresponds to G_{Kf_1}; a component which inactivates with a time constant of 2 sec at $E = 0$ mV (curve *d*) and corresponds to G_{Kf_2}. The inactivation induced by conditioning depolarizations to 0 mV develops in two phases corresponding respectively to the inactivation of G_{Kf_1} and G_{Kf_2} (*B*). The inactivation induced by conditioning depolarizations to −40 mV develops in one phase corresponding to the inactivation of G_{Kf_1} (*C*, 5). When tested after the shutting off of G_{Kf_2} by a transient repolarization to −40 mV, the inactivation induced by conditioning depolarizations to 0 mV develops in one phase corresponding to the inactivation of G_{Kf_1} (*C*, 4). Fibre: 7-6-9.

first method is twice that of the second one. In order to minimize errors due to the running down of the fibres, the second method was thus preferred.

The voltage dependence of the fast K^+ conductance activation was studied from fast instantaneous currents recorded after 200 msec depolarizing pulses of various amplitudes (pulse protocol 1, Fig. 7). The fast conductance–voltage curve obtained systematically showed a bend near $E = -40\ mV$ (curve *a* Fig. 7*A*). Assuming that this bend does not reflect a series resistance artifact, one explanation for the G_{Kf}–V curve is that it consists of the sum of two superimposed conductance–voltage curves reflecting two fast K^+ currents which activate over different voltage ranges (e.g. G_{Kf_1} in the voltage range -80 to -40 mV and G_{Kf_2} in the voltage range -40 to $+50$ mV).

The view that there may be two distinct types of fast K^+ channels is also supported by the data of Schwarz & Vogel (1971) who showed that, in normal Ringer, the K^+ current inactivates in two phases. However, it was shown in the preceding paper that, in the first tens of milliseconds after a depolarization, the decrease in I_K recorded in normal Ringer is probably due to a decrease in driving force rather than inactivation of the conductance. Thus it is important to known whether, in the absence of significant changes in driving force, the fast K^+ current still inactivates in two phases. This was tested in the experiment presented Fig. 7 *B* using the pulse protocol 3. The instantaneous fast K^+ current (I_{Kf}) recorded in isotonic KCl Ringer at the holding potential is plotted against the duration of the conditioning depolarization at $E = 0$ mV. The decline in I_{Kf} can be described by two exponential functions of time, thus confirming the conclusions of Schwarz & Vogel. After correction for the temperature, the values of the time constants (2 and 45 sec) are comparable to the values presented by Schwarz & Vogel.

The next step of this investigation was to find out whether the two inactivation phases of the fast K^+ current are respectively related to the two hypothetical conductance–voltage curves (G_{Kf_1} and G_{Kf_2}). If this hypothesis were true, then, because of the large difference between the two inactivation time constants, it should be possible to completely suppress the conductance component which inactivates quickly while only partly suppressing the component which inactivates slowly. the G_{Kf}–V curve calculated from the instantaneous fast K^+ current recorded upon repolarization should then not present a bend near -40 mV and should correspond to only one of the two hypothetical G_{Kf}–V curves (G_{Kf_1} or G_{Kf_2}) partially decreased.

Inactivation was induced by depolarizations to 0 mV lasting 3·7 sec, followed by 200 msec pulses of varying amplitude. The tail current was recorded upon repolarization. The instantaneous fast current was obtained after subtraction of the instantaneous extrapolated slow current from the peak of the total tail current. The fast conductance-voltage curve (curve *b*, Fig. 7*A*), obtained from the variation of the instantaneous fast tail current as a function of the conditioning voltage, is a pure sigmoid curve corresponding to G_{Kf_1} partly inactivated. This result agrees with the hypothesis that the two phases of inactivation represent two classes of fast K^+ channels which correspond to the two limbs of the activation curve for the fast K^+ conductance. Scaling curve *b* by a constant factor (to correct for partial inactivation of G_{Kf_1} assuming that activation and inactivation develop in parallel) so as to superimpose on curve *a* between -90 and -40 mV gives the curve *c*, describing the voltage dependence of G_{Kf_1} at the end of 200 msec depolarizing pulses. The difference

between the curve *a* and *c* gives the curve *d* describing the voltage dependence of G_{Kf_2} at the end of 200 msec depolarizing pulses.

From these results, it appears that the fast K^+ conductance is composed of two components: a conductance (G_{Kf_1}) activating in the voltage range -80 to -30 mV and inactivating slowly ($\tau = 45$ sec at 0 mV); a conductance (G_{Kf_2}) activating in the voltage range -40 to $+50$ mV, and inactivating quickly ($\tau = 2$ sec at 0 mV). Based on these conclusions, one can make two predictions. (i) If one applies a conditioning pulse to 0 mV to activate and inactivate G_{Kf_1} and G_{Kf_2}, followed by a 100 msec repolarization to a membrane potential equal or more negative than -40 mV, to de-activate G_{Kf_2} (double conditioning pulse, protocol 4 in Fig. 7), then the instantaneous fast K^+ tail current recorded upon repolarization to the holding potential should decrease with the duration of the conditioning pulse at 0 mV in only one slow exponential phase reflecting the inactivation of G_{Kf_1} alone. (ii) The inactivation of the conductance induced by conditioning depolarizations to a membrane potential more negative than about -40 mV (pulse protocol 5) should develop in only one slow exponential phase, since only G_{Kf_1} is activated here. These predictions were tested in the experiment presented Fig. 7*C*. With the double conditioning pulse protocol, the kinetics of the conductance inactivation can indeed be described by only one exponential function, whose time constant (44 sec) is close to that calculated for the slow inactivation phase obtained with the single conditioning pulse protocol 3. With a conditioning depolarization to -40 mV, the kinetics of the conductance inactivation can also be described by only one exponential function (time constant: 25 sec). These results are in agreement with the predictions and strongly support the idea that the fast K^+ conductance is composed of two individual components (G_{Kf_1} and G_{Kf_2}), corresponding to two classes of fast K^+ channels.

Properties of the fast K^+ channels

It has been shown above that increasing the external K^+ concentration increases the slow K^+ conductance without affecting its voltage dependence. It was of interest to know whether similar conclusions can be drawn for the fast K^+ conductances. The fast K^+ conductances were calculated in 117 and 60 mM-K solutions, for fibres exhibiting no significant K^+ accumulation, from the fast tail current (total tail current minus extrapolated slow tail current) recorded at -90 mV after 200 msec conditioning pulses of various amplitudes. Fig. 8*A* shows the total fast K^+ conductance as a function of voltage during the conditioning pulse for both solutions. The conductance is higher in 117 mM-K than in 60 mM-K. After scaling the curve obtained in 60 mM-K by a constant factor, so it is superimposed on the curve obtained in 117 mM-K, it appears that the effect of the external K^+ concentration on the total fast conductance is independant of voltage. From the same experiment, it also appears that the external K^+ concentration has no effect on the time course of the fast tail current upon repolarization after activation of the conductances by a 200 ms depolarization to 0 mV (Fig. 8*B*). These results imply that (i) the voltage and time dependent gating processes of the K^+ channels are not controlled by K^+ ions; (ii) the only effects of $[K]_0$ are on the maximum conductance and are quantitatively identical on G_{Kf_1} and G_{Kf_2}.

After a conditioning depolarization to 0 mV, the time course of the fast tail current

represents (in the absence of noticeable K^+ accumulation) the shutting off of both fast conductances (G_{Kf_1} and G_{Kf_2}). One can ask whether the closing kinetics of both types of fast channels are identical. To answer this question, the fast tail current was recorded after activation of different proportions of fast conductances. It appears (Fig. 8*C*) that the time course of the fast tail current is independent of the relative proportion of G_{Kf_1} and G_{Kf_2} activated. Consequently, it can be concluded that the kinetics of shutting off of both fast types of K^+ channels are identical at -90 mV.

A semilogarithmic plot of the fast tail current following a depolarization to -40 mV (Fig. 8*D*) indicates that its time course can be described by two exponential functions. Since virtually no G_{Kf_2} is activated at -40 mV, it is unlikely that the two

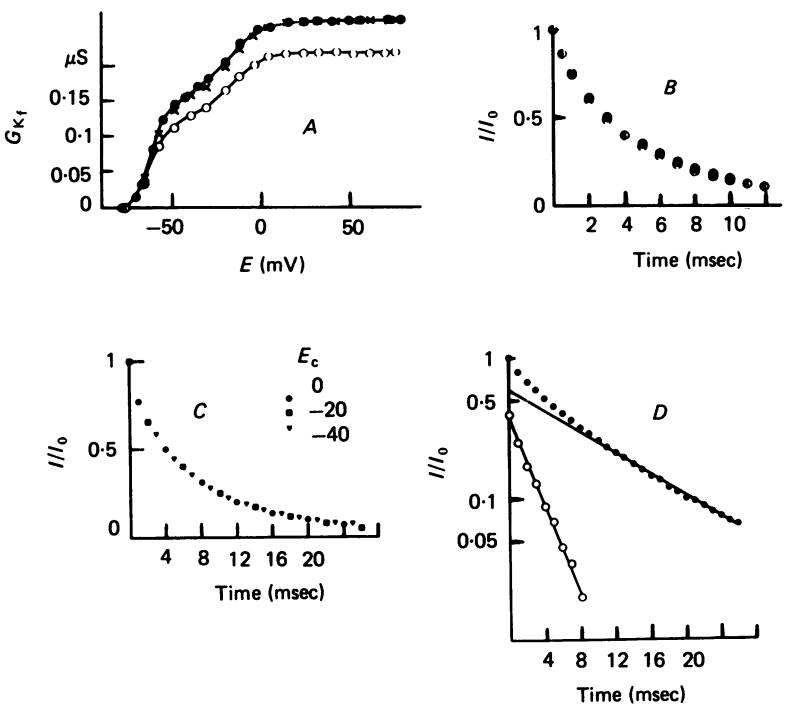

Fig. 8. The total fast K^+ conductance was calculated in 117 and 60 mM-K from instantaneous fast current (total instantaneous current minus instantaneous extrapolated slow tail current) recorded at -90 mV after activation of the conductance by 100 msec conditioning depolarizations of various amplitudes. *A*, fast K^+ conductance–voltage curves in 117 mM-K (●) and 60 mM-K (○). The crosses represent the conductance in 60 mM-K scaled by 1·2. Note that a decrease in the external K^+ concentration induced a decrease of the total fast conductance but changes neither the proportion of both fast conductances amplitude nor alters their voltage dependence. Fibre: 14–9–9. *B*, fast tail current in 117 mM-K (●) and 60 mM-K (○) arising at repolarization (-90 mV) after a conditioning depolarization to 0 mV. Note that the time course of the fast tail current is not altered by a change in the external K^+ concentration. Fibre: 14–9–9. *C*, fast tail current in 117 mM-K arising at repolarization (-90 mV) after conditioning depolarizations to -40, -20 and 0 mV. Note that the time course of the tail current is independent of the amplitude of the conditioning depolarization. Fibre: 10–7–9*b*. *D*, semilogarithmic plot of the fast tail current in 117 mM-K arising at repolarization (-90 mV) after a conditioning depolarization to -40 mV. The time course of the tail current can be described by the sum of two exponential functions of time. Fibre: 10–7–9*b*.

exponentials represent the closing of two types of channels. A more likely explanation would be that both fast conductances are determined by a multi-step process (see Discussion). Since the fast tail current kinetics at −90 mV were the same following activation of different proportions of G_{Kf_1} and G_{Kf_2} (Fig. 8*C*) the off rate constants for the two channels should be very similar at −90 mV.

Variation of K^+ conductances with the external K^+ concentration

Earlier (Dubois & Bergman, 1977), it was concluded that the K^+ concentration dependence of the K^+ conductance could be described as resulting from a reaction between K^+ ions and membrane sites controlling the opening of the channels. In that

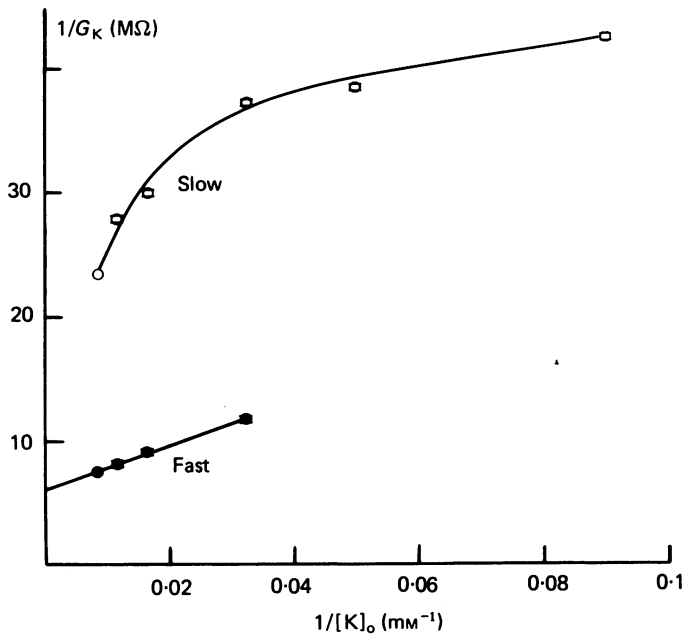

Fig. 9. The fast K^+ conductance was calculated from fast instantaneous current (instantaneous total current minus instantaneous extrapolated slow tail current) recorded at −90 mV after 200 ms conditioning depolarizations to −30 mV. Means and standard errors calculated from data obtained on three different preparations and normalized to the mean of the values in 117 mM-K. The slow K^+ conductance was calculated either from instantaneous slow current recorded in the presence of 4AP (1 mM) at −90 mV after 700 msec conditioning depolarizations to +30 mV in 117, 60, 31, 17 and 2·5 mM-K or from instantaneous extrapolated slow tail current recorded at −90 mV after 200 msec conditioning depolarizations to −30 mV in 117, 88, 60 and 31 mM-K. Means and standard errors calculated from data obtained on six different preparations (three in the presence of 4-AP) and normalized to the mean of the values in 117 mM-K. The straight line is the linear regression calculated from fast conductance values. The curve through the points (slow conductance) was drawn by eye.

study, the K^+ conductance was considered to correspond to one uniform population of K^+ channels. The aim of the following analysis was to determine whether similar conclusions can be proposed for both slow and fast K^+ channels. To minimize accumulation, the fast K^+ conductance was calculated from the instantaneous fast

tail current (peak of the total tail current minus extrapolated slow tail current) arising at the end of 200 msec depolarizing pulses to −30 mV in 117, 88, 60 and 31 mM-K solutions. The slow K^+ conductance was calculated either from extrapolated slow tail current obtained in the same conditions as the fast tail currents or from instantaneous slow current recorded after 800 msec depolarizing pulses to +30 mV in 117, 60, 31, 17 and 2·5 mM-K solutions containing 1 mM-4-AP. In 2·5 and 17 mM-K, the actual outside concentrations, calculated from the reversal potential of the instantaneous current, were slightly larger than concentrations in the bulk solutions (11 mM instead of 2·5 mM and 20 mM instead of 17 mM, mean of three experiments), reflecting a small accumulation induced by the outward slow K^+ current. Owing to the absence of voltage dependence of the effect of $[K]_0$ on the conductances (see Figs 4 and 8, the slow and fast conductances calculated in the presence of the different K^+ concentrations with 4-AP (three experiments) or without 4-AP (three experiments) were respectively normalized to the mean slow and fast conductances calculated in 117 mM-K. Fig. 9 shows the relationship $1/G_K$ *vs.* $1/[K]_0$ for the fast and the slow conductances. For the fast K^+ conductance, the experimental points are distributed along a straight line suggesting a one to one saturating reaction of the channels with K^+ ions. In contrast, for the slow conductance, the experimental points are not distributed along a straight line. It might be argued that the different variation of the slow and fast conductances as a function of the external K^+ concentration is only apparent and due to the fact that the fast conductance was not calculated for K^+ concentrations below 31 mM while the slow conductance was calculated for a larger range of K^+ concentrations. This seems unlikely since even in the range 117–31 mM, the experimental points for the slow conductance do not follow a straight line. The difference between the fast and slow conductance-concentration relationships seems more likely related to a difference in the channels.

Physiological significance of fast and slow K^+ channels

In recent work (Krylov & Makovsky, 1978), it has been suggested that the decrease in firing frequency during a sustained stimulus (spike frequency adaptation) was due to a K^+ current flowing through slow channels. On the basis of this hypothesis, the well known differences in spike frequency adaptation of motor and sensory fibres was attributed to a difference in slow K^+ channels densities. The motor fibres which respond to a sustained stimulus by producing only one spike would have a larger density of slow K^+ channels than sensory fibres which respond to a sustained stimulus by producing a train of spikes. Furthermore, it is well known that the time courses of the action potential of both type of fibres are different, i.e. the initial rate of decline of the action potential is faster in sensory than in motor fibres. Differences between the K^+ conductances of the two types of fibres were reported earlier (Bergman & Stämpfli, 1966; Bretag & Stämpfli, 1975). The conductance–voltage curves of sensory fibres compared to those of motor fibres appears to be shifted towards positive voltages. It was of interest to see whether these observations could be explained by a difference in the proportion of the three types of K^+ channels.

The total conductance and the relative amplitude of slow and total fast conductances on one hand and the relative amplitude of fast-1 and fast-2 conductances on the other hand were calculated in 117 mM-K on motor and sensory fibres from the tail current

arising at repolarization after a 100 ms depolarization to +30 mV. Assuming that the internal K^+ concentration, the axoplasmic resistance (through which the current is measured as a voltage drop) and the nodal area are identical on both fibres, it appears (Table 1) that the total conductance and the relative amplitudes of slow and fast conductances are identical on both types of fibres. However, a significant difference

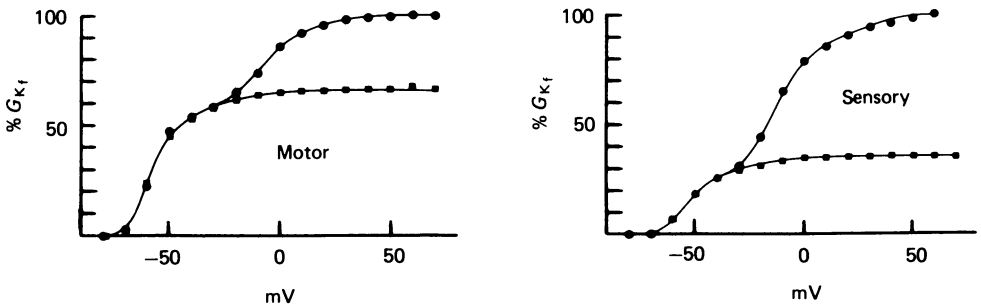

Fig. 10. The fast K^+ conductances were calculated from instantaneous fast current (instantaneous total current minus instantaneous extrapolated slow current) recorded at −90 mV after 100 msec conditioning depolarizations of various amplitudes. The values of the total fast conductance (circles) were obtained using a holding potential of −90 mV. The values of the fast-1 conductance (squares) were calculated from the values obtained using a holding potential of 0 mV and scaled by a constant factor (1·45 for the motor fibre and 1·33 for the sensory fibre) (see text and Fig. 7 for procedure details). Note that the relative amplitudes of fast 1 and fast 2 conductances are different in motor and sensory fibres. Motor fibre: 6–11–9. Sensory fibre: 28–11–9.

TABLE 1. Total (T), fast (f) and slow (s) K^+ conductances amplitudes in motor and sensory fibres calculated from instantaneous currents recorded in 117 mM-K at −90 mV after 100 msec depolarizations to +30 mV

Fibre type	$G_{KT} \mp$ S.E. μsec	$G_{Ks} \mp$ S.E. (% G_{KT})	$G_{Kf} \mp$ S.E. (% G_{KT})	$G_{Kf_1} \mp$ S.E. (% G_{Kf})	$G_{Kf_2} \mp$ S.E. (% G_{Kf})
Motor eight experiments	0·319 ∓ 0·027	18 ∓ 1	82 ∓ 1	61 ∓ 3	39 ∓ 3
Sensory three experiments	0·307 ∓ 0·083	19 ∓ 5	81 ∓ 5	35 ∓ 2	65 ∓ 2

appears between the relative amplitudes of fast-1 and fast-2 conductances. This is illustrated in Fig. 10 which represents for both types of fibres the variation with voltage of the total fast and the fast-1 conductances calculated as in Fig. 7 (pulse protocols 1 and 2). On motor fibres, the maximum G_{Kf_1} is slightly larger than the maximum G_{Kf_2} (50–65 % for G_{Kf_1}). In contrast, on sensory fibres, the maximum G_{Kf_1} is noticeably smaller than the maximum G_{Kf_2} (30–40 % for G_{Kf_1}). These differences can account for the 'positive' shift of the conductance–voltage curve observed on sensory fibres compared to motor fibres since for membrane potentials more negative than −10 mV, the total fast conductance (which mainly represents the classical conductance studied in earlier works) is smaller in sensory than in motor fibres.

The present observations contradict the hypothesis that the spike frequency adaptation is due to the slow K^+ current since the relative amplitudes of the slow K^+

conductance are identical in motor and sensory fibres. From the present work, it is concluded that on sensory fibres, the phenomenon of repetitive firing is related to the small fast K^+ conductance in the negative voltage range associated with a marked non-inactivatable Na^+ conductance (Dubois & Bergman, 1975). Bretag & Stämpfli (1975) and Y. Palti (personal communication) observed that the activation time constant of the K^+ conductance is smaller in sensory than in motor fibres at positive membrane potentials. This was not investigated in the present work. It would suggest that the kinetics of the fast-2 conductance change is faster than those of the fast-1 conductance in the positive voltage range while they are identical for negative membrane potentials (see Fig. 8*C*). Such differences associated with the different amplitude of both fast conductances could account for the faster initial rate of repolarization of sensory fibres.

At the level of the resting potential (−70 mV), the relative amplitude of the slow K^+ conductance is relatively high (see Fig. 4*A*) and comparable to the amplitude of the fast conductance on motor fibres (see Fig. 7*A*). On the contrary, in sensory fibres, the fast K^+ conductance is practically nil at the resting potential (see Fig. 10*B*) which should only be governed by the leakage, the slow K^+ and Na^+ resting conductances. Van den Berg *et al.* (1977) suggested that the slow K^+ conductance is less sensitive to tetraethylammonium than the fast K^+ conductance; this would explain the smaller effect of TEA on the resting potential of sensory fibres compared to motor fibres (Bergman & Stämpfli, 1966).

To test this hypothesis, the effect of external TEA was investigated in 117 mM-K solutions on fast and slow conductances calculated from tail currents arising at repolarization after conditioning depolarizations to 0 mV. Both fast and slow currents are abolished in the presence of 5×10^{-2} M-TEA. With 3×10^{-4} M-TEA, the fast and slow conductances are respectively reduced to $34{\cdot}0 \mp 2{\cdot}2$ and $47{\cdot}7 \mp 3{\cdot}3$% (ten measurements on five fibres) of their original values. This result is in agreement with the observation of Van den Berg *et al.* (1977) and furnish a further evidence of the existence of different types of K^+ channels. The relative effects of TEA on both fast-1 and fast-2 conductances were not systematically investigated. However, a few measurements revealed that the affinity of both types of fast channels for TEA are identical.

DISCUSSION

The existence of different types of K^+ channels has been demonstrated in molluscan neurones (Neher, 1971; Thompson, 1977) in skeletal muscle (Adrian, Chandler & Hodgkin, 1970) and cardiac muscle (Noble & Tsien, 1969). In myelinated nerve fibres, the existence of several types of K^+ channels has been suggested by several authors but without direct evidence. In the present work, strong arguments are presented showing that the K^+ channel population of the Ranvier node membrane is composed of three distinct classes. A non-inactivatable K^+ current, flowing through slow K^+ channels can be separated from the total K^+ current by three different methods): (i) exponential extrapolation of the slow phase of the tail current; (ii) full inactivation of the fast current; (iii) complete blockage of the fast current by 4-aminopyridine. The fast K^+ current can be decomposed into two distinct components by two methods: (i) full inactivation of one fast conductance (G_{Kf_2}) and only partial

inactivation of the other fast conductance (G_{Kf_1}), which activate respectively in different voltage ranges (Fig. 7*A*, curves *a* and *b*); (ii) inactivation of only one conductance (G_{Kf_1}), tested after activation of either G_{Kf_1} or G_{Kf_1} and G_{Kf_2} and deactivation of G_{Kf_2}. The fact that one or two of the three K^+ components can be altered independently of the others suggests that the different components do not correspond to different and interconvertible conductances states of the same channels.

The slow and fast K^+ channels are quite different. Except that they are both specific for K^+ ions and blocked by TEA, they exhibit very different behaviour with respect to voltage, time and 4-AP. On the other hand, the structures of the fast-1 and fast-2 channels do not seem to be very different. The different voltage dependences of the fast-1 and fast-2 channels could be because they are located in different membrane areas voltage clamped at different levels or that their voltage sensors are situated more or less deeply within the membrane.

Because the slow K^+ current cannot be specifically blocked, the activation time course of the fast conductance should be calculated after subtraction of the slow current recorded in the presence of 4-AP from the total current (see Fig. 3*A*). This method was not systematically used. However, taking account of the large differences in time course and amplitude of both fast and slow current, it can be assumed that at all potentials, the activation of the total conductance mainly reflects the activation of the fast conductance and thus can be described by the equation (see the preceding paper)

$$G_{Kf} = G_{Kf_\infty}\,(1-e^{-(t-\delta t)}/\tau).$$

Upon repolarization, the de-activation of the fast conductance can be described by the sum of two exponential functions of time (see Fig 8*D*). The results presented in Fig. 5 of the preceding paper and in Fig. 8*C* of the present paper suggest that the kinetics of activation and de-activation of both fast-1 and fast-2 conductances are identical. The observation that the de-activation of the fast-conductances can be described by the sum of the two exponential functions of time, associated with the existency of a delay in the activation, strongly suggests that the opening and closing of the fast channels follow a two step transition.

In agreement with earlier results (Dubois & Bergman, 1977), it is concluded that the K^+ conductances (fast and slow) are functions of the external K^+ concentration. However, in contrast with the results of 1977, it is concluded here that the effect of the external K^+ concentration is independent of voltage (see Figs 4 and 8) and that the only effect of $[K]_o$ is on the maximum conductances. The reason for this discrepancy seems to be due to the fact that the effect of the external K^+ concentration on fast and slow conductances are quantitatively different (see Fig. 9). Thus by considering the total conductance, Dubois & Bergman (1977), reached different conclusions from those arrived at here by considering each conductance individually.

The evidence of the existence of three different types of K^+ channels were obtained here in high K^+ media. The last point which must be discussed is whether similar conclusions can be drawn from data obtained in normal K^+ solutions. In 2·5 mM-K, the slow K^+ current can be seen in the presence of 4-AP or after complete inactivation of fast conductances. The separation of the slow K^+ current from the total tail current

is impossible, even after correction for the change in driving force, because the shutting off of the conductance reflects both the change in voltage gating processes and in maximum conductances (via a change in external K^+ concentration). As, at the present time, no specific blocker was found for the slow K^+ current, the fast K^+ conductances cannot be separated from the total conductance. However, the development of the inactivation in two phases (Schwarz & Vogel, 1971) and the existence of a bend near -30 mV in the total conductance–voltage curve (see Fig. 2*C* of the preceding paper) confirm the presence of two fast conductances.

I am indebted to D. Attwell, C. Bergman, M. F. Schneider and S. Siegelbaum for helpful discussions and criticisms of the manuscript.

REFERENCES

ADRIAN, R. H., CHANDLER, W. K. & HODGKIN, A. L. (1970). Slow changes in potassium permeability in skeletal muscle. *J. Physiol.* **208**, 645–668.

ATTWATER, I., DAWSON, C. M., RIBALET, B. & ROJAS, E. (1979). Potassium permeability activated by intracellular calcium ion concentration in the pancreatic β-cell. *J. Physiol.* **288**, 575–588.

ATTWELL, D., DUBOIS, J. M. & OJEDA, C. (1980). Fully activated potassium current–voltage relationship in the Ranvier node. *Pflügers Arch.* **384**, 49–56.

BEGENISICH, T. (1979). Conditioning hyperpolarization-induced delays the potassium channels of myelinated nerve. *Biophys. J.* **27**, 257–266.

BERGMAN, C. & STÄMPFLI, R. (1966). Différence de perméabilité des fibres nerveuses myélinisées sensorielles et motrices à l'ion potassium. *Helv. physiol. pharmac. Acta* **24**, 247–258.

BRETAG, A. H. & STÄMPFLI, R. (1975). Differences in action potentials and accomodation of sensory and motor myelinated nerve fibres as computed on the basis of voltage clamp data. *Pflügers Arch.* **354**, 257–271.

COLE, K. S. & MOORE, J. W. (1960). Potassium ion current in the squid giant axon: dynamic characteristic. *Biophys. J.* **1**, 1–14.

DUBOIS, J. M. (1981). Simultaneous changes in the equilibrium potential and potassium conductance in voltage clamped Ranvier node in the frog. *J. Physiol.* **318**, 279–295.

DUBOIS, J. M. & BERGMAN, C. (1975). Late sodium current in the node of Ranvier. *Pflügers Arch.* **357**, 145–148.

DUBOIS, J. M. & BERGMAN, C. (1977). The steady-state potassium conductance of the Ranvier node at various external K-concentrations. *Pflügers Arch.* **370**, 185–194.

ILYIN, V. I., KATINA, I. E., LONSKII, A. V., MAKOVSKY, V. S. & POLISHCHUK, E. V. (1977). Evidence of the existence of two independent components of potassium current in the Ranvier node of the frog *Rana ridibunda*. *Dokl. Akad. Nauk SSSR* **234**, 1467–1470.

KRYLOV, B. V. & MAKOVSKY, V. S. (1978). Spike frequency adaptation in amphibians sensory fibres is probably due to slow K-channels. *Nature, Lond.* **275**, 549–551.

MEECH, R. W. (1978). Calcium-dependent potassium activation in nervous tissues. *Annu. Rev. Biophys. & Bioeng.* **7**, 1–18.

MEVES, H. & PICHON, Y. (1977). The effect of internal and external 4-aminopyridine on the potassium currents in intracellularly perfused squid giant axons. *J. Physiol.* **268**, 511–532.

NEHER, E. (1971). Two fast transient current components during voltage clamp on snail neurones. *J. gen. Physiol.* **58**, 36–53.

NOBLE, D., TSIEN, R. W. (1969). Outward membrane currents activated in the plateau range of potentials in cardiac purkinje fibres. *J. Physiol.* **200**, 205–231.

PALTI, Y., GANOT, G. & STÄMPFLI, R. (1976). Effect of conditioning potential on potassium current kinetics in the frog node. *Biophys. J.* **16**, 262–273.

SCHWARZ, J. R. & VOGEL, W. (1971). Potassium inactivation in single myelinated nerve fibre of *Xenopus laevis*. *Pflügers Arch.* **330**, 61–73.

THOMPSON, S. H. (1977). Three pharmacologically distinct potassium channels in molluscan neurones. *J. Physiol.* **265**, 465–488.

ULBRICHT, W. & WAGNER, H. H. (1976). Block of potassium channels of the nodal membrane by 4-aminopyridine and its partial removal on depolarization. *Pflügers Arch.* **367**, 77–87.

VAN DEN BERG, R. J., SIEBENGA, E. & DE BRUIN, G. (1977). Potassium ion noise currents and inactivation in voltage-clamped node of Ranvier. *Nature, Lond.* **265**, 177–179.

YEH, J. Z., OXFORD, G. S., WU, C. H. & NARAHASHI, T. (1976). Dynamics of aminopyridine block of potassium channels in squid axon membrane. *J. gen. Physiol.* **68**, 519–535.